Helical Mathieu and parabolic localized pulses

Josue Davila-Rodriguez and Julio C. Gutiérrez-Vega*

Photonics and Mathematical Optics Group, Tecnológico de Monterrey, Monterrey, México 64849
**Corresponding author: juliocesar@itesm.mx*

Received August 16, 2007; accepted August 31, 2007;
posted September 7, 2007 (Doc. ID 86457); published October 10, 2007

Using suitable polychromatic superpositions of helical Mathieu and parabolic nondiffracting beams, we study for the first time, to the best of our knowledge, the higher-order helical Mathieu X waves and the traveling and stationary parabolic X waves. The mathematical and physical properties of these new kinds of localized pulses are discussed. © 2007 Optical Society of America

OCIS codes: 260.1960, 350.5500, 050.1960.

1. INTRODUCTION

Localized pulses are broadband wave-packet solutions of the wave equation that have been widely studied since the introduction by Lu and Greenleaf of the so-called X waves [1,2]. Over the last 15 years, the theory of localized pulses has been developed and experimentally verified in the fields of acoustics [1,2], microwaves [3], and optics [4–7] for a variety of extended spectral functions. On the other hand, nondiffracting beams are monochromatic solutions of the wave equation that propagate indefinitely in free space without changing their transverse intensity distribution [8,9]. Optical generation and characterization of nondiffracting beams are now well established, and new beam structures and applications are actively being reported [10]. Four fundamental families of nondiffracting beams are known: plane waves in Cartesian coordinates, Bessel beams in circular coordinates [8,9], Mathieu beams in elliptic coordinates [11,12], and parabolic beams in parabolic coordinates [13,14]. Here we use the term "fundamental" to refer to a complete family of beams that constitutes a basis for expanding any arbitrary nondiffracting beam with the same transverse spatial frequency.

The connection between localized pulses and nondiffracting beams arises from the fact that the former can be constructed with a suitable polychromatic superposition of the latter [5,6]. Until now, plane waves and Bessel beams have served as the standard basis to build X waves [2,5,6]; however, this construction can certainly also be realized using Mathieu and parabolic nondiffracting beams. In this direction, in a recent paper, Dartora and Hernandez-Figueroa [15] reported for the first time, as far as we know, an X wave based on the superposition of zeroth-order, even Mathieu beams, obtaining a localized pulse that lacked the typical rotational symmetry found in Bessel-based X waves.

In this paper, we show the general method for obtaining localized pulses based on the polychromatic superposition of fundamental families of nondiffracting beams and then introduce for the first time, to the best of our knowledge, helical Mathieu X waves and traveling and stationary parabolic X waves. The physical properties of these localized pulses are discussed. This approach provides alternative insight into the physics of X waves and sheds light on the strong connection of these waves to the nondiffracting solutions used in optics. Finally, we remark that this work consolidates and extends previous studies on zeroth-order Mathieu localized pulses [15].

2. LOCALIZED PULSES IN TERMS OF NONDIFFRACTING BEAMS

We begin by writing the wave equation in free space for the time-varying scalar field $U(\mathbf{r}_t,z,t)$,

$$\left(\nabla_t^2+\frac{\partial^2}{\partial z^2}-\frac{1}{c^2}\frac{\partial^2}{\partial t^2}\right)U(\mathbf{r}_t,z,t)=0, \tag{1}$$

where $\mathbf{r}_t=(x,y)=(r\cos\theta,r\sin\theta)$ denotes the position at the transverse plane, ∇_t^2 is the transverse Laplacian operator, and c is the light speed.

Localized waves are defined through the condition of uniform propagation $U(\mathbf{r}_t,z,t)=U(\mathbf{r}_t,z-vt)$, where v is the velocity of propagation of the wave field. This condition leads to the known Fourier representation $\tilde{U}(\mathbf{k}_t,k_z,\omega)$ of the X waves given by [5,6]

$$\tilde{U}(\mathbf{k}_t,k_z,\omega)=G(\phi,\omega)\delta\left(k_z-\frac{\omega}{c}\cos\alpha\right)\delta\left(k_t-\frac{\omega}{c}\sin\alpha\right), \tag{2}$$

where ω is the angular frequency, $\mathbf{k}_t=(k_x,k_y)=(k_t\cos\phi,k_t\sin\phi)$ denotes the position at the transverse plane in the $\mathbf{k}$ space, and δ is the Dirac delta function. The wave vectors $\mathbf{k}$ of the X wave lie on a cone of top angle 2α that opens from the k_z axis in $\mathbf{k}$ space. The constituent plane waves propagate at speed c along the cone but their interference pattern has a superluminal velocity $v=c/\cos\alpha$. The complex amplitude function $G(\phi,\omega)$ is arbitrary and determines the transverse shape and the localization properties of the beam.

X waves in space are obtained by inverse Fourier transforming Eq. (2):

$$U(\mathbf{r}_t,\zeta)=\int_0^\infty \mathrm{d}\omega \exp\left[i\left(\frac{\omega}{c}\cos\alpha\right)\zeta\right] \times \int_{-\pi}^{\pi}\mathrm{d}\phi G(\phi,\omega)\exp\left[i\left(\frac{\omega}{c}\sin\alpha\right)r\cos(\phi-\theta)\right], \tag{3}$$

where $\zeta\equiv z-vt$ is the longitudinal coordinate of a moving frame traveling at speed v along the z axis. Throughout the paper, the fields $U(\mathbf{r}_t,z,t)$ are restricted to positive frequencies ω only.

It is convenient to write the angular spectrum in the separable form

$$G(\phi,\omega)=A(\phi)f(\omega). \tag{4}$$

This separation is reasonable for the following reasons: (a) writing $G(\phi,\omega)$ as a product only assumes a decoupling between the spectral composition of the light source and the spatial structure of the macroscopic field; (b) in the case when these functions are not decoupled, arbitrary $G(\phi,\omega)$ can be built with a proper superposition of functions with the separable form, and (c) writing the function as a product allows for a representation of X waves in terms of fundamental families of nondiffracting beams, whose properties have been explored in several coordinate systems [8,11,13]. For example, the choice $G(\phi,\omega)=\exp(im\phi)f(\omega)$ leads to the well-known mth-order X waves based on Bessel beams $J_m(\kappa_t r)\exp(im\theta)$.

By defining the transverse and longitudinal wave numbers $\kappa_t\equiv(\omega/c)\sin\alpha$ and $\kappa_z\equiv(\omega/c)\cos\alpha$ and using Eq. (4), then $U(\mathbf{r}_t,\zeta)$ [Eq. (3)] takes the form

$$U(\mathbf{r}_t,\zeta)=\int_0^\infty f(\omega)\Phi(\mathbf{r}_t,\omega)\exp(i\kappa_z\zeta)\mathrm{d}\omega, \tag{5}$$

where

$$\Phi(\mathbf{r}_t,\omega)\equiv\int_{-\pi}^{\pi}\mathrm{d}\phi A(\phi)\exp[i\kappa_t(\omega)r\cos(\phi-\theta)], \tag{6}$$

is a solution of the two-dimensional Helmholtz equation [10]

$$[\nabla_t^2+\kappa_t(\omega)^2]\Phi=0, \tag{7}$$

and physically describes the transverse field of an ideal scalar nondiffracting beam with transverse wavenumber $\kappa_t\equiv(\omega/c)\sin\alpha$. The expressions in Eqs. (3) and (6) are completely general in the sense that they do not depend on a particular coordinate system. Since the spectrum $G(\phi,\omega)$ is arbitrary, an infinite number of transverse profiles can be obtained.

It is clear from Eq. (5) that an X wave is obtained from a polychromatic superposition of pure nondiffracting beams with transverse and longitudinal wave numbers given by κ_t and κ_z, respectively. The wave is stationary in a moving frame which travels along the z axis with constant speed $v=c/\cos\alpha$. In Sections 3 and 4 we apply the formalism developed in this section to introduce localized X waves based on Mathieu and parabolic beams.

3. HELICAL MATHIEU PULSES

Mathieu beams constitute a complete and orthogonal family of nondiffracting beams that are solutions of the wave equation in elliptic coordinates [11,12,16,17]. Recently, these beams have been applied for example to photonic lattices [18] and the transfer of orbital angular momentum using optical tweezers [19,20]. Gaussian apodized Mathieu beams, which carry a finite power and can be generated experimentally to a very good approximation, have been already reported in free space [21,22] and through *ABCD* optical systems [23,24].

A. Spectral Integral Representation

To construct X waves based on helical Mathieu beams we set the spatial part of the spectrum to be

$$A_m^{\pm}(\phi,\varepsilon)=\mathrm{ce}_m(\phi,\varepsilon)\pm i\mathrm{se}_m(\phi,\varepsilon), \tag{8}$$

where $\mathrm{ce}_m(\cdot)$ and $\mathrm{se}_m(\cdot)$ are the even and odd angular Mathieu functions of mth-order and ellipticity parameter $\varepsilon\geq 0$. The positive and negative signs correspond to positive and negative helicity of the spectrum and eventually determine the direction of the orbital angular momentum carried by the wave field.

Replacement of Eq. (8) into Eq. (6) yields the transverse field of the helical Mathieu beams, namely

$$\Phi_m^{\pm}(\mathbf{r}_t,\omega)=\mathcal{C}_m\mathrm{Je}_m(\xi,\varepsilon)\mathrm{ce}_m(\eta,\varepsilon)\pm i\mathcal{S}_m\mathrm{Jo}_m(\xi,\varepsilon)\mathrm{se}_m(\eta,\varepsilon), \tag{9}$$

where $\mathrm{Je}_m(\cdot)$ and $\mathrm{Jo}_m(\cdot)$ are the mth-order even and odd radial Mathieu functions, and $\mathcal{C}_m$ and $\mathcal{S}_m$ are normalization factors to ensure that the even and odd parts carry the same power. In Eq. (9), the radial $\xi\in[0,\infty)$ and angular $\eta\in[0,2\pi)$ elliptic coordinates are related to the Cartesian coordinates according to

$$x=h\cosh\xi\cos\eta, \tag{10a}$$

$$y=h\sinh\xi\sin\eta, \tag{10b}$$

where $h=2\sqrt{\varepsilon}/\kappa_t=2\sqrt{\varepsilon}(c/\omega)\csc\alpha$ is the semifocal distance of the elliptic coordinate system. The transverse distribution of the helical Mathieu beams [Eq. (9)] is characterized by a set of confocal elliptic rings whose eccentricity is determined by the parameter ε. [19] The special case when $\varepsilon=0$ corresponds to the known mth-order Bessel beams $J_m(\kappa_t r)\exp(\pm im\theta)$ for which the spectrum [Eq. (8)] is $A_m^{\pm}(\phi,0)=\cos m\phi\pm i\sin m\phi$.

Substitution of Eq. (9) into Eq. (5) leads to the general integral representation for helical Mathieu based X wave of mth-order

$$U_m^{\pm}(\mathbf{r}_t,\zeta)=\int_0^\infty f_m(\omega) \times[\mathcal{C}_m\mathrm{Je}_m(\xi,\varepsilon)\mathrm{ce}_m(\eta,\varepsilon)\pm i\mathcal{S}_m\mathrm{Jo}_m(\xi,\varepsilon)\mathrm{se}_m(\eta,\varepsilon)] \times\exp(i\kappa_z\zeta)\mathrm{d}\omega. \tag{11}$$

Every nondiffracting X wave can be obtained from waves of this form by suitably weighing and summing over m.

B. Orthogonality of Helical Mathieu X Waves

We now turn to consider the orthogonality condition for helical Mathieu X waves. At a fixed time, the scalar product of two waves is defined by

$$\langle U_m|U_n\rangle = \int_{-\infty}^{\infty} U_m^*(\mathbf{r}_t,z,t)U_n(\mathbf{r}_t,z,t)\mathrm{d}x\mathrm{d}y\mathrm{d}z. \quad (12)$$

Substituting the Fourier representation of the wave [Eq. (3)] into the scalar product, integrating over a cylinder of radius R, and substituting the angular spectrum of the helical Mathieu X waves [Eq. (8)], we obtain

$$\langle U_m|U_n\rangle = \frac{R\tan\alpha}{2\pi^2}\int_0^{\infty}\mathrm{d}\omega\omega f_m^*(\omega)f_n(\omega) \times \int_{-\pi}^{\pi}[\mathrm{ce}_m(\phi)\mp i\mathrm{se}_m(\phi)][\mathrm{ce}_n(\phi)\pm i\mathrm{se}_n(\phi)]\mathrm{d}\phi. \quad (13)$$

Since the angular Mathieu functions $\mathrm{ce}_m(\phi)$ and $\mathrm{se}_m(\phi)$ satisfy the same orthogonality relations as their trigonometric counterparts $\cos\phi$ and $\sin\phi$ [25,26], then Eq. (13) reduces to

$$\langle U_m|U_n\rangle = \frac{R\tan\alpha}{2\pi}\delta_{m,n}\int_0^{\infty}\mathrm{d}\omega\omega f_m^*(\omega)f_n(\omega), \quad (14)$$

where $\delta_{m,n}$ is the Kronecker delta symbol. Note that two helical Mathieu X waves with the same order are orthogonal inside the volume enclosed by the cylinder R if the integral in Eq. (14) vanishes. The inner product diverges as $R\to\infty$, which accounts for the fact that ideal Mathieu beams and X waves are not square integrable over all space.

C. Helical Mathieu X Waves in Terms of Bessel X Waves

The two-dimensional Helmholtz equation [Eq. (7)] can be solved in several orthogonal coordinate systems using the separation of variables method [26]. This fact leads to complete and orthogonal families of eigenfunctions of the two-dimensional Helmholtz equation and eventually of X waves. In this sense, helical Mathieu X waves can also be expressed as a summation of the standard X waves based on Bessel beams of the form

$$\mathrm{BB}_n^{\pm}(r,\theta) = J_n(\kappa_t r)\exp(\pm in\theta). \quad (15)$$

From [27] we know that monochromatic even and odd Mathieu beams admit of the Bessel expansions

$$\mathrm{Je}_m(\xi,\varepsilon)\mathrm{ce}_m(\eta,\varepsilon) = \sum_{n=0}^{\infty}\mathcal{A}_n^{(m)}J_n(\kappa_t r)\cos(n\theta), \quad (16a)$$

$$\mathrm{Jo}_m(\xi,\varepsilon)\mathrm{se}_m(\eta,\varepsilon) = \sum_{n=0}^{\infty}\mathcal{B}_n^{(m)}J_n(\kappa_t r)\sin(n\theta), \quad (16b)$$

where $\mathcal{A}_n^{(m)}$ and $\mathcal{B}_n^{(m)}$ are the expansion coefficients whose explicit expressions can be found in [27,28]. Replacing into Eq. (9) and using the intermediate results

$$J_n(\kappa_t r)\cos(n\theta) = \tfrac{1}{2}(\mathrm{BB}_n^+ + \mathrm{BB}_n^-), \quad (17)$$

$$J_n(\kappa_t r)\sin(n\theta) = \tfrac{1}{2i}(\mathrm{BB}_n^+ - \mathrm{BB}_n^-), \quad (18)$$

we obtain the transverse field of the helical Mathieu beam in terms of a summation of Bessel beams, namely

$$\Phi_m^+(\mathbf{r}_t,\omega) = \sum_{n=0}^{\infty}[D_n^+\mathrm{BB}_n^+(r,\theta) + D_n^-\mathrm{BB}_n^-(r,\theta)], \quad (19)$$

where

$$D_n^{\pm} = \tfrac{1}{2}(\mathcal{C}_m\mathcal{A}_n^{(m)} \pm \mathcal{S}_m\mathcal{B}_n^{(m)}). \quad (20)$$

Finally, substitution into Eq. (11) produces

$$U_m^+(\mathbf{r}_t,\zeta) = \sum_{n=0}^{\infty}[D_n^+\mathrm{X}_n^+(r,\theta,\zeta) + D_n^-\mathrm{X}_n^-(r,\theta,\zeta)],$$

where

$$\mathrm{X}_n^{\pm}(r,\theta,\zeta) = \int_0^{\infty}\mathrm{d}\omega f_m(\omega)\mathrm{BB}_n^{\pm}(r,\theta)\exp(i\kappa_z\zeta), \quad (21)$$

is the well-known integral expression for the nth-order Bessel X wave [5,6].

D. Three-Dimensional Distribution of the Helical Mathieu X Waves

In this paper we study the three-dimensional distribution of the helical Mathieu X waves using a spectral function of the general form

$$f(\omega) = \omega^p(\omega-\omega_{\min})(\omega_{\max}-\omega)\exp(-\mu\omega). \quad (22)$$

The spectrum contains four parameters: (i) p and μ control the skewness of the distribution (see Fig. 1), and (ii) $\omega_{\min}$ and $\omega_{\max}$ adjust the bandwidth of the function to the range $[\omega_{\min},\omega_{\max}]$ since the form of the polynomial forces the end points to be zero. The spectral distribution in Eq. (22) can be visualized as a superposition of two spectral functions of the standard form (polynomial in ω) $\times\exp(-\mu\omega)$ which is the usual form adopted for the spectral dependency of the X waves based on Bessel beams [5–7].

The amplitude of a fifth-order helical Mathieu X wave in the planes $y=0$ and $\zeta=[-2,-1,0,1,2]$ μm is illustrated in Fig. 2(a). The conical angle α is 15° and the frequency spectrum is given by Eq. (22) with the parameters corresponding to the function $f_I(\omega)$ included in the caption of

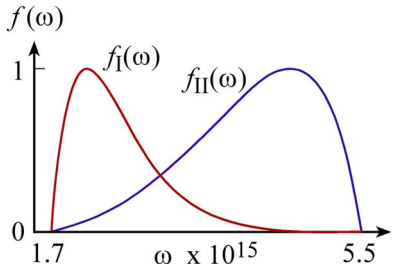

Fig. 1. (Color online) Spectral functions given by Eq. (22) with $p=1$, $\omega_{\min}=1.71\times10^{15}$ rad/s and $\omega_{\max}=5.54\times10^{15}$ rad/s. For the spectrum f_I $\mu=2.13\times10^{-15}$ m^{-1}, and for f_{II} $\mu=-8.53\times10^{-16}$ s. The spectra are normalized such that the maximum of the spectral function is unity.

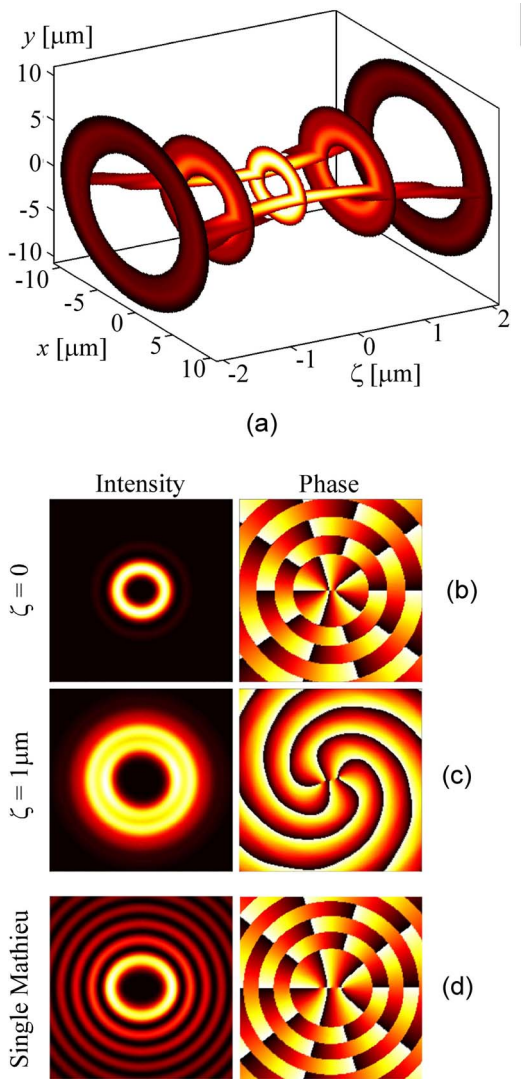

Fig. 2. (Color online) (a) Amplitude of a fifth-order helical Mathieu X wave in the planes $y=0$ and $\zeta=[-2,-1,0,1,2]$ μm using the spectral function $f_I(\omega)$ shown in Fig. 1. (b) and (c) Transverse intensity and phase distributions of the wave at $\zeta=0$ and $\zeta=1$ μm. (d) Intensity and phase of a Mathieu beam whose frequency ω corresponds to the maximum value of the spectral function f_I.

Fig. 1. The three-dimensional field distribution was obtained by solving Eq. (11) at 201 transverse planes evenly spaced through the range $|\zeta| \leq 2$ μm. The wave is localized and remains invariant in a coordinate system $(x,y,\zeta=z-vt)$ that propagates in the z direction at a superluminal velocity $v=c/\cos\alpha$. The Mathieu X wave is of infinite transverse extent and it has a divergent total energy, which are typical properties of the ideal X wave [5–7].

In Fig. 2(b) we show the transverse intensity and phase distributions of the wave at $\zeta=0$. The pattern is characterized by a well-defined bright elliptic ring and a phase that rotates following an elliptic trajectory. For $m>1$, the phase exhibits m in-line vortices, each with unitary topological charge such that the total charge (along a closed trajectory enclosing all the vortices) is m. Unlike Bessel X waves, the Mathieu X waves are not rotationally symmetric with respect to the propagation axis.

The intensity and phase of the wave at $\zeta=1$ μm are included in Fig. 2(c). The spirallike structure of the phase is an indication that the X wave acquires a spherical wavefront as the longitudinal coordinate increases. The topological charge remains constant at any transverse plane. To compare the transverse pattern of the Mathieu X wave [Fig. 2(b)] with respect to the monochromatic Mathieu beam, in Fig. 2(d) we show the intensity and phase of a Mathieu beam whose frequency ω corresponds to the maximum value of the spectral function f_I in Fig. 1. While for the monochromatic wave the energy is shared between several elliptic rings, for the polychromatic wave the energy is much more concentrated in a single and well-defined elliptic ring.

The spectral function $f_I(\omega)$ used for the Mathieu X wave shown in Fig. 2 is skewed to the lower frequencies. For comparison purposes, in Fig. 3 we show the same fifth-

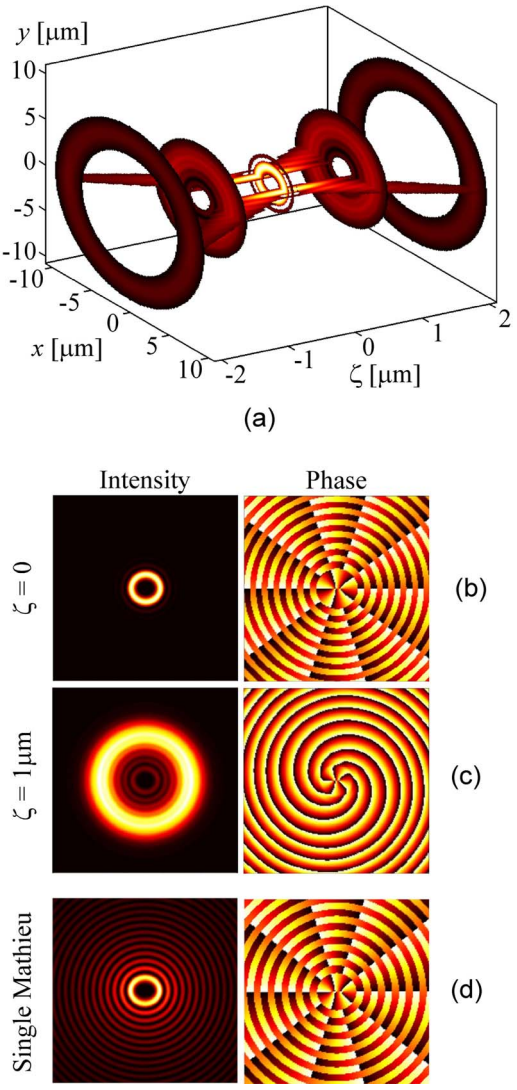

Fig. 3. (Color online) (a) Amplitude of a fifth-order helical Mathieu X wave in the planes $y=0$ and $\zeta=[-2,-1,0,1,2]$ μm using the spectral function $f_{II}(\omega)$ shown in Fig. 1. (b) and (c) Transverse intensity and phase distributions of the wave at $\zeta=0$ and $\zeta=1$ μm. (d) Intensity and phase of a Mathieu beam whose frequency ω corresponds to the maximum value of the spectral function f_{II}.

order helical Mathieu X wave but now we are using the spectral function $f_{II}(\omega)$ which is skewed to higher frequencies (see Fig. 1). The separation between consecutive rings is now smaller than in Fig. 2 because the transverse spatial frequency κ_t of each spectral Mathieu component is proportional to ω, and we now have more contributions at larger frequencies.

4. PARABOLIC X WAVES

We now turn to consider parabolic nondiffracting beams, which constitute the fourth family of fundamental nondiffracting beams [13,14] and can also serve as a basis to construct localized X waves. The transverse structure of the parabolic beams is described by the parabolic cylinder functions, and, contrary to Bessel or Mathieu beams, their eigenvalues are continuous instead of discrete.

A. Spectral Integral Representation

To construct X waves based on parabolic beams we set the spatial part of the spectrum to be

$$A^{\pm}(\phi) = A_e(\phi;a) \pm iA_o(\phi;a), \tag{23}$$

where

$$A_e(\phi;a) = \sqrt{\frac{\pi}{2|\sin\phi|}}\exp\left(ia\ln\left|\tan\frac{\phi}{2}\right|\right), \tag{24}$$

$$A_o(\phi;a) = \frac{1}{i}\begin{cases} -A_e(\phi;a), & \phi\in(-\pi,0) \\ A_e(\phi;a), & \phi\in(0,\pi) \end{cases}, \tag{25}$$

and $a\in(-\infty,\infty)$ is the continuous parabolicity parameter that plays the role of an order. Replacement of Eq. (23) into Eq. (6) yields the transverse field of the parabolic beams [13,14], namely

$$\Phi_m^{\pm}(\mathbf{r}_t,\omega) = \Phi_m^e(\mathbf{r}_t,\omega) \pm i\Phi_m^o(\mathbf{r}_t,\omega), \tag{26}$$

$$\Phi_m^{\pm}(\mathbf{r}_t,\omega) = |\Gamma_1|^2 \mathrm{P}_e(\sigma\xi;a)\mathrm{P}_e(\sigma\eta;-a) \pm i2|\Gamma_3|^2\mathrm{P}_o(\sigma\xi;a)\mathrm{P}_o(\sigma\eta;-a), \tag{27}$$

where $\sigma\equiv(2\kappa_t)^{1/2}$, $\Gamma_1\equiv\Gamma(1/4+ia/2)$, and $\Gamma_3\equiv\Gamma(3/4+ia/2)$. In Eq. (27), $\mathrm{P}_e(v;a)$ and $\mathrm{P}_o(v;a)$ are the even and odd real solutions of the parabolic cylinder differential equation $(d^2/dx^2+x^2/4-a)\mathrm{P}(x;a)=0$, and the parabolic cylindrical coordinates $\mathbf{r}_t=(\xi,\eta)$ are defined as $x=(\eta^2-\xi^2)/2$, $y=\xi\eta$, where $\xi\in[0,\infty)$ and $\eta\in(-\infty,\infty)$. The stationary solutions Φ_m^e and Φ_m^o are called the even and odd parabolic beams, respectively.

Figure 4 shows the transverse intensity and phase distributions for an even and a traveling parabolic beam with $a=-1.618$. For $a<0$, the transverse intensity pattern of the parabolic beams consists of well-defined nondiffracting parabolic fringes with a dark parabolic region surrounding the negative x axis [13]. For the even and odd parabolic beams the intensity and phase patterns are invariant under propagation; however, for the traveling parabolic beams when observed at a fixed transverse plane the phase travels along confocal parabolic trajectories around the semiplane $(x<0,z)$ for $a<0$.

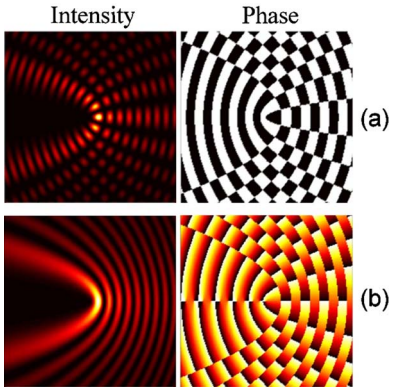

Fig. 4. (Color online) Intensity and phase transverse distribution of an even and a traveling parabolic nondiffracting beam.

Substitution of Eq. (27) into Eq. (5) leads to the general integral representation for parabolic X waves

$$U_a^{\pm}(\mathbf{r}_t,\zeta) = U_a^e(\mathbf{r}_t,\zeta) \pm iU_a^o(\mathbf{r}_t,\zeta), \tag{28}$$

$$U_a^{\pm}(\mathbf{r}_t,\zeta) = \int_0^{\infty} f_a(\omega)[|\Gamma_1|^2\mathrm{P}_e(\sigma\xi;a)\mathrm{P}_e(\sigma\eta;-a) \pm i2|\Gamma_3|^2\mathrm{P}_o(\sigma\xi;a)\mathrm{P}_o(\sigma\eta;-a)]\exp(i\kappa_z\zeta)\mathrm{d}\omega. \tag{29}$$

Every nondiffracting X wave can be obtained from parabolic X waves of this form by suitably weighing and integrating over the continuous order a.

B. Three-Dimensional Distribution of Parabolic X Waves

To gain insight into parabolic X waves, in Fig. 5 we show the amplitude of an even parabolic X wave $U_a^e(\mathbf{r}_t,\zeta)$ in the planes $y=0$ and $\zeta=[-2,-1,0]$ μm for $a=-1.618$ and a conical angle $\alpha=15^\circ$. The frequency spectrum is given by Eq. (22) with the parameters corresponding to the function $f_{II}(\omega)$ included in the caption of Fig. 1 with $\mu=-9.26\times10^{-16}$ s. Like Mathieu X waves, the parabolic X waves are of infinite transverse extent and have a divergent total energy.

For the particular case shown in Fig. 5 the even parabolic X wave comes from the polychromatic superposition of real parabolic nondiffracting beams $U_a^e(\mathbf{r}_t,\zeta)$ with an even parity about the x axis; therefore the beam does not carry orbital angular momentum and the pattern remains symmetrical about the x axis for any longitudinal position ζ. The phase structure of the wave shown in Fig. 5(d) suggests that the field at the plane $\zeta=0$ reduces to a purely real function resembling the original even parabolic beam shown in Fig. 4(a). Outside the plane $\zeta=0$, the wave acquires a spherical phase front leading to an intrincate structure of vortices.

The three-dimensional distribution of a complex traveling parabolic X wave is depicted in Fig. 6 at the planes $\zeta=[-2,-1,0]$ μm. All the beam parameters are the same as for the corresponding even component shown in Fig. 5. The spatial distribution was obtained by solving Eq. (29) at 201 transverse planes evenly spaced through the range $|\zeta|\le2$ μm. The propagating behavior of the traveling parabolic X waves is expected to be different from that of the stationary even and odd parabolic X waves. Because

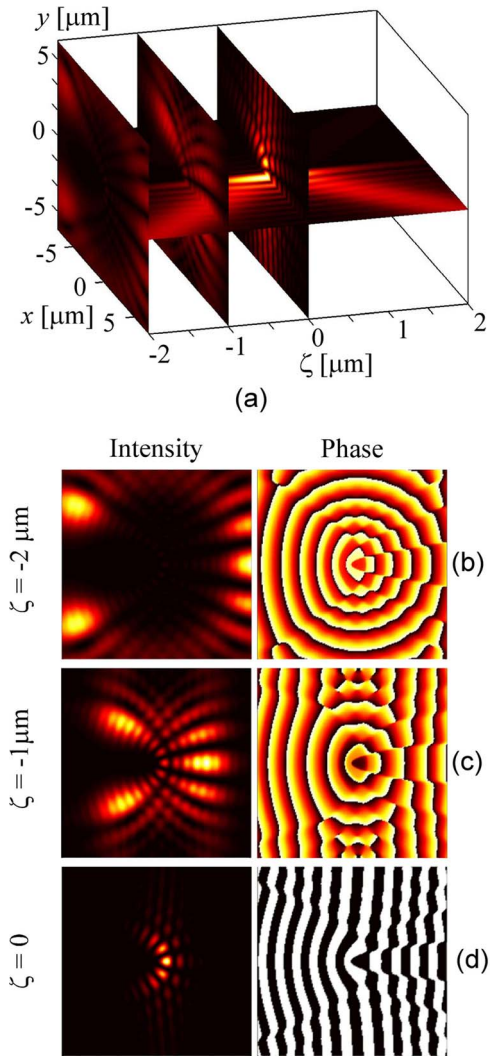

Fig. 5. (Color online) Amplitude and phase of an even parabolic X wave in the planes $y=0$ and $\zeta=[-2,-1,0]\,\mu$m using the spectral function $f_{II}(\omega)$ shown in Fig. 1.

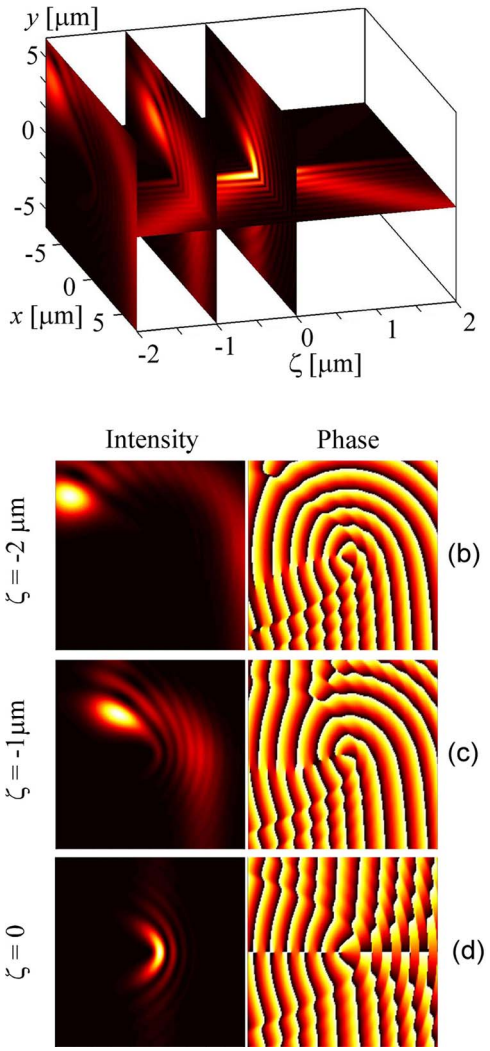

Fig. 6. (Color online) Amplitude and phase of a traveling parabolic X wave in the planes $y=0$ and $\zeta=[-2,-1,0]\,\mu$m using the spectral function $f_{II}(\omega)$ shown in Fig. 1.

of its complex phase distribution, transverse energy flow must occur along parabolic trajectories. Such behavior for the transverse energy flow is clearly observed in the image sequence shown in Fig. 6. Note that the energy flows within the parabolic nodal lines around the negative x axis, and that the field is symmetrical about the x axis at the plane $\zeta=0$.

The results shown in Fig. 6 are of particular interest because they clearly illustrate the behavior of the transverse energy flow occurring in the traveling parabolic X waves. Even though this effect also takes place in Bessel X waves and helical Mathieu X waves for which their nodal lines are closed, in the case of the parabolic X waves the nodal lines never close making this effect more significant.

5. CONCLUSIONS

We have shown the general method for constructing localized pulses based on the polychromatic superposition of fundamental families of nondiffracting beams. We put emphasis on the helical Mathieu X waves of higher order and the traveling and stationary parabolic X waves. The particular mathematical and physical properties of these two new localized waves were discussed and exemplified with some illustrative examples and plots. Several applications for the new Mathieu and parabolic X wave pulses could be explored in high-speed optical processing and communications, medical real-time imaging, optical microlithography, and acoustic waves in crystals [29].

ACKNOWLEDGMENTS

This research was partially supported by Consejo Nacional de Ciencia y Tecnología of México grant 42808, and by the Tecnológico de Monterrey Research Chair in Optics grant CAT–007.

REFERENCES

1. J. Lu and J. F. Greenleaf, "Ultrasonic nondiffracting transducer for medical imaging," IEEE Trans. Ultrason. Ferroelectr. Freq. Control **37**, 438–447 (1990).
2. J. Lu and J. F. Greenleaf, "Nondiffracting X waves: exact solutions to free-space scalar wave equation and their finite

aperture realizations," IEEE Trans. Ultrason. Ferroelectr. Freq. Control **39**, 19–31 (1992).
3. E. Recami, M. Zamboni-Rached, K. Z. Nóbrega, C. A. Dartora, and H. E. Hernández-Figueroa, "On the localized superluminal solutions to the Maxwell equations," IEEE J. Sel. Top. Quantum Electron. **9**, 59–73 (2003).
4. P. Saari and K. Reivelt, "Evidence of X-shaped propagation-invariant localized light waves," Phys. Rev. Lett. **79**, 4135–4138 (1997).
5. J. Fagerholm, A. T. Friberg, J. Huttunen, D. P. Morgan, and M. M. Salomaa, "Angular-spectrum representation of nondiffracting X waves," Phys. Rev. E **54**, 4347–4352 (1996).
6. J. Salo, J. Fagerholm, A. T. Friberg, and M. M. Salomaa, "Unified description of nondiffracting X and Y waves," Phys. Rev. E **62**, 4261–4275 (2000).
7. J. Salo, A. T. Friberg, and M. M. Salomaa, "Orthogonal X waves," J. Phys. A **34**, 9319–9327 (2001).
8. J. Durnin, "Exact solutions for nondiffracting beams. I. The scalar theory," J. Opt. Soc. Am. A **4**, 651–654 (1987).
9. J. Durnin, J. J. Micely Jr., and J. H. Eberly, "Diffraction-free beams," Phys. Rev. Lett. **58**, 1499–1501 (1987).
10. Z. Bouchal, "Nondiffracting optical beams: physical properties, experiments, and applications," Czech. J. Phys. **53**, 537–578 (2003).
11. J. C. Gutiérrez-Vega, M. D. Iturbe-Castillo, and S. Chávez-Cerda, "Alternative formulation for invariant optical fields: Mathieu beams," Opt. Lett. **25**, 1493–1495 (2000).
12. J. C. Gutiérrez-Vega, M. D. Iturbe-Castillo, G. A. Ramírez, E. Tepichín, R. M. Rodríguez-Dagnino, S. Chávez-Cerda, and G. H. C. New, "Experimental demonstration of optical Mathieu beams," Opt. Commun. **195**, 35–40 (2001).
13. M. A. Bandres, J. C. Gutiérrez-Vega, and S. Chávez-Cerda, "Parabolic nondiffracting optical wave fields," Opt. Lett. **29**, 44–46 (2004).
14. C. López-Mariscal, M. A. Bandres, S. Chávez-Cerda, and J. C. Gutiérrez-Vega, "Observation of parabolic nondiffracting optical fields," Opt. Express **13**, 2364–2369 (2005).
15. C. A. Dartora and H. E. Hernández-Figueroa, "Properties of a localized Mathieu pulse," J. Opt. Soc. Am. A **21**, 662–667 (2004).
16. C. A. Dartora, M. Zamboni-Racheda, K. Z. Nobrega, E. Recami, and H. E. Hernández-Figueroa, "General formulation for the analysis of scalar diffraction-free beams using angular modulation: Mathieu and Bessel beams," Opt. Commun. **222**, 75–80 (2003).
17. A. Chafiq, Z. Hricha, and A. Belafhal, "Paraxial propagation of Mathieu beams through an apertured *ABCD* optical system," Opt. Commun. **253**, 223–230 (2005).
18. Y. V. Kartashov, A. A. Egorov, V. A. Vysloukh, and L. Torner, "Shaping soliton properties in Mathieu lattices," Opt. Lett. **31**, 238–240 (2006).
19. S. Chávez-Cerda, M. J. Padgett, I. Allison, G. H. C. New, J. C. Gutiérrez-Vega, A. T. O'Neil, I. MacVicar, and J. Courtial, "Holographic generation and orbital angular momentum of high-order Mathieu beams," J. Opt. B: Quantum Semiclassical Opt. **4**, S52–S57 (2002).
20. C. López-Mariscal, J. C. Gutiérrez-Vega, G. Milne, and K. Dholakia, "Orbital angular momentum transfer in helical Mathieu beams," Opt. Express **14**, 4182–4187 (2006).
21. J. C. Gutiérrez-Vega and M. A. Bandres, "Helmholtz–Gauss waves," J. Opt. Soc. Am. A **22**, 289–298 (2005).
22. C. López-Mariscal, M. A. Bandrés, and J. C. Gutiérrez-Vega, "Observation of the experimental propagation properties of Helmholtz-Gauss beams," Opt. Eng. (Bellingham) **45**, 068001 (2006).
23. A. Chafiq, Z. Hricha, and A. Belafhal, "A detailed study of Mathieu–Gauss beams propagation through an apertured *ABCD* optical system," Opt. Commun. **265**, 594–602 (2006).
24. M. Guizar-Sicairos and J. C. Gutiérrez-Vega, "Generalized Helmholtz-Gauss beam and its transformation by paraxial optical systems," Opt. Lett. **31**, 2912–2914 (2006).
25. J. C. Gutiérrez-Vega, R. M. Rodríguez-Dagnino, M. A. Meneses-Nava, and S. Chávez-Cerda, "Mathieu functions, a visual approach," Am. J. Phys. **71**, 233–242 (2003).
26. M. Abramowitz and I. Stegun, *Handbook of Mathematical Functions* (Dover, 1964).
27. J. C. Gutiérrez-Vega and M. A. Bandres, "Normalization of the Mathieu–Gauss optical beams," J. Opt. Soc. Am. A **24**, 215–220 (2007).
28. I. S. Gradshteyn and I. M. Ryzhik, *Table of Integrals, Series, and Products* (Academic, 2000).
29. J. Salo, J. Fagerholm, A. T. Friberg, and M. M. Salomaa, "Nondiffracting bulk-acoustic X waves in crystals," Phys. Rev. Lett. **83**, 1171–1174 (1999).